

Interferometry at 337 μm on a Tokamak Plasma

P. BROSSIER AND R. A. BLANKEN

Abstract—The Alcator electron density ($10^{13} < n_e < 10^{14} \text{ cm}^{-3}$) has been measured with a 337- μm Mach-Zender interferometer. A detailed description of the interferometer is given. Results are discussed and compared with microwave interferometry data.

I. INTRODUCTION

THE classic method to measure the electron density of a plasma is to measure the phase shift induced in an electromagnetic beam. The wavelength of the probing beam must be adapted to the plasma characteristics: plasma density n_e and plasma size d . One must have a frequency low enough to have a measurable phase shift but larger than the maximum value of the electron plasma frequency, so that the probing beam is not cut off. Accordingly, optical and near infrared frequencies have been used to probe high-density ($n_e > 10^{16} \text{ cm}^{-3}$) plasmas. On the other hand, microwave interferometry [1] is a standard diagnostic method for low-density plasmas ($n_e < 10^{13} \text{ cm}^{-3}$). The advent of thermonuclear plasmas with densities in the intermediate range ($10^{13} < n_e < 10^{15} \text{ cm}^{-3}$) requires the development of interferometers using submillimeter wavelengths. In this paper we describe an interferometer working at 337 μm which has been built to measure the electron density of Alcator. Alcator [2] is a high magnetic field Tokamak where n_e is expected to be in the range $5 \cdot 10^{13} < n_e < 10^{14} \text{ cm}^{-3}$. In Section II we state the conditions to be satisfied by the probing beam to fit this range of density. Section III is a description of the interferometer. We present the experimental results in Section IV.

II. MICROWAVE INTERFEROMETRY VERSUS FAR-INFRARED INTERFEROMETRY

1) For the beam to be transmitted through the plasma, its frequency f_b must be larger than the maximum electron plasma frequency f_{eo}

$$f_b > f_{eo} = 8979 n_{eo}^{1/2} \text{ Hz} \quad (1)$$

where n_{eo} is the maximum (on-axis) plasma density in cm^{-3} . Table I gives the cutoff density

$$n_{co} = 1.24 \times 10^{-8} f_b^2 \text{ cm}^{-3} \quad (2)$$

for four different probing wavelengths.

Manuscript received May 11, 1974. This work was supported in part by the U.S. Atomic Energy Commission under Contract AT(11-1)-3070.

P. Brossier was with the Massachusetts Institute of Technology, Cambridge, Mass. 02139. He is now with Association Euratom-CEA, Fontenay aux Roses, France.

R. A. Blanken is with the Massachusetts Institute of Technology, Cambridge, Mass. 02139.

TABLE I

λ_b (mm)	f_b (GHz)	n_{co} (cm^{-3})
10	30	$1.12 \cdot 10^{13}$
4	75	$6.98 \cdot 10^{13}$
2	150	$2.79 \cdot 10^{14}$
0.337	890	$9.82 \cdot 10^{15}$

Although standard microwave interferometry (at $\lambda = 2 \text{ mm}$) can be used to measure the on-axis density we will show below that it is difficult to determine the density profile using microwave interferometry. Fig. 1 shows the range of observable densities using millimeter and submillimeter wavelengths. The line $n = n_{co}$ corresponds to relation (2).

Note that for densities such that $n_{co}/3 \lesssim n_{eo} < n_{co}$, the phase shift becomes a nonlinear function of the density. Specifically, for a parabolic density profile $n_e(r) = n_{eo}(1 - r^2/a^2)$, it can be shown that the phase shift for the ordinary mode

$$\frac{\Delta\phi}{2\pi} = \frac{1}{\lambda_b} \int_{-a}^{+a} \left[1 - \left(1 - \frac{n_e(r)}{n_{co}} \right)^{1/2} \right] dr \quad (3)$$

is equal to

$$\left(\frac{\Delta\phi}{2\pi} \right)_{n_{eo} < n_{co}} = \frac{a}{\lambda_b} \left[1 - \frac{1}{2} \left[(n_{co}/n_{eo})^{1/2} - (n_{eo}/n_{co})^{1/2} \right] \cdot \ln \left(\frac{1 + (n_{eo}/n_{co})^{1/2}}{1 - (n_{eo}/n_{co})^{1/2}} \right) \right] \quad (4)$$

which in the low-density limit $n_{eo} \ll n_{co}/3$ becomes the usual linear phase shift

$$\left(\frac{\Delta\phi}{2\pi} \right)_{n_{eo} \ll n_{co}} = \frac{2}{3} \frac{a}{\lambda_b} \frac{n_{eo}}{n_{co}}. \quad (5)$$

The ratio of (4) to (5) is given by

$$f(y) = \frac{3}{2y} \left[1 - \frac{1}{2} \left(\frac{1}{y^{1/2}} - y^{1/2} \right) \ln \left(\frac{1 + y^{1/2}}{1 - y^{1/2}} \right) \right] \quad (6)$$

where $y \equiv n_{eo}/n_{co}$; $f(y)$ varies from 1 at $y = 0$ to 1.5 at $y = 1$. In other words, using (5) to unfold the data can lead to an overestimation of the peak density by as much as 50 percent. Care must thus be exerted when using a probing frequency such that $n_{co}/3 < n_{eo} < n_{co}$. Fig. 1 also shows some expected linear phase shifts, the density being averaged over a 20-cm plasma diameter.

2) The plasma acts as a lens on the probing beam. Although the rays going through the center of the plasma

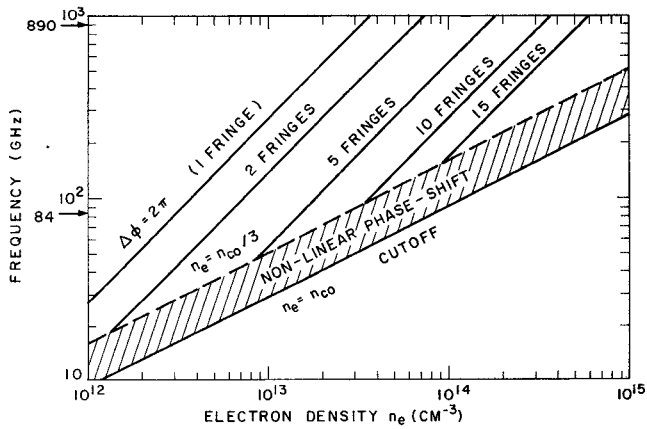


Fig. 1. Range of observable densities versus probing frequency.

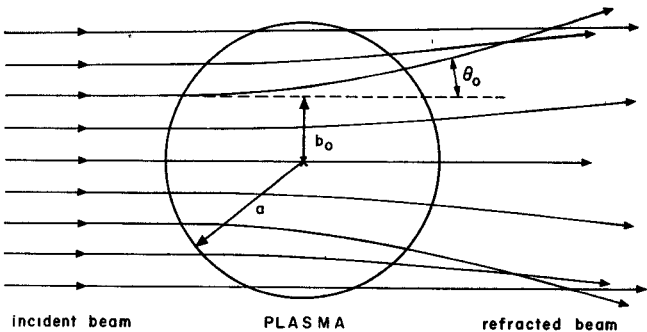


Fig. 2. Refraction by the plasma.

density profile are not deviated, those having an impact parameter $b_0 \simeq a/4$ (Fig. 2) undergo a significant deviation. Shmoys [3] has shown that for a wide range of near parabolic profiles the maximum angle of deviation θ_0 is well approximated by

$$\theta_0 = \sin^{-1} (n_{eo}/n_{co}) = \sin^{-1} (8.96 \times 10^{-16} n_{eo} \lambda^2) \text{ rad} \quad (7)$$

where the density n_{eo} is in cm^{-3} and the wavelength λ is in centimeters. [Condition (1) is obviously supposed satisfied.] Fig. 3 shows the variation of θ_0 with the probing wavelength for different maximum electron densities. For standard microwave wavelengths ($\lambda \gtrsim 2 \text{ mm}$) and for typical Tokamak densities ($n_{eo} \gtrsim 6 \times 10^{13} \text{ cm}^{-3}$), θ_0 becomes quite large ($\theta_0 > 10^\circ$), and the positioning of the receiving horn becomes an impossible task (the density has a time varying profile). Since the detailed knowledge of the density profile and of its time evolution is quite important in the study of Tokamak containment laws, the development of interferometers working at shorter wavelengths is required. For Alcator we developed a Mach-Zender interferometer working at $337 \mu\text{m}$, which gives a measurable phase shift, and for which $\theta_0 < 1^\circ$ at $n_{eo} = 10^{14} \text{ cm}^{-3}$.

III. DESCRIPTION OF THE INTERFEROMETER

Although submillimeter interferometry is not entirely new, it has never been applied to a plasma of thermonuclear quality. We will show in Subsection III-1) the difficult experimental conditions introduced by the sophisticated technology and high magnetic field of Alcator. Subsection III-2) is a description of the laser used as

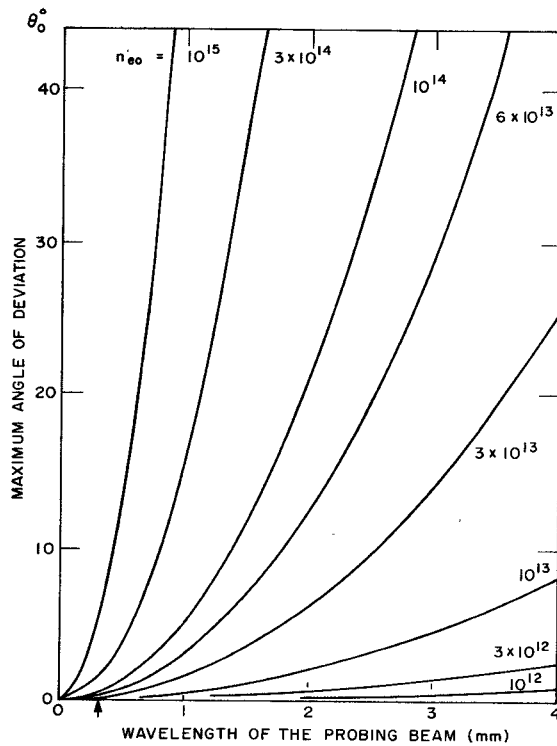
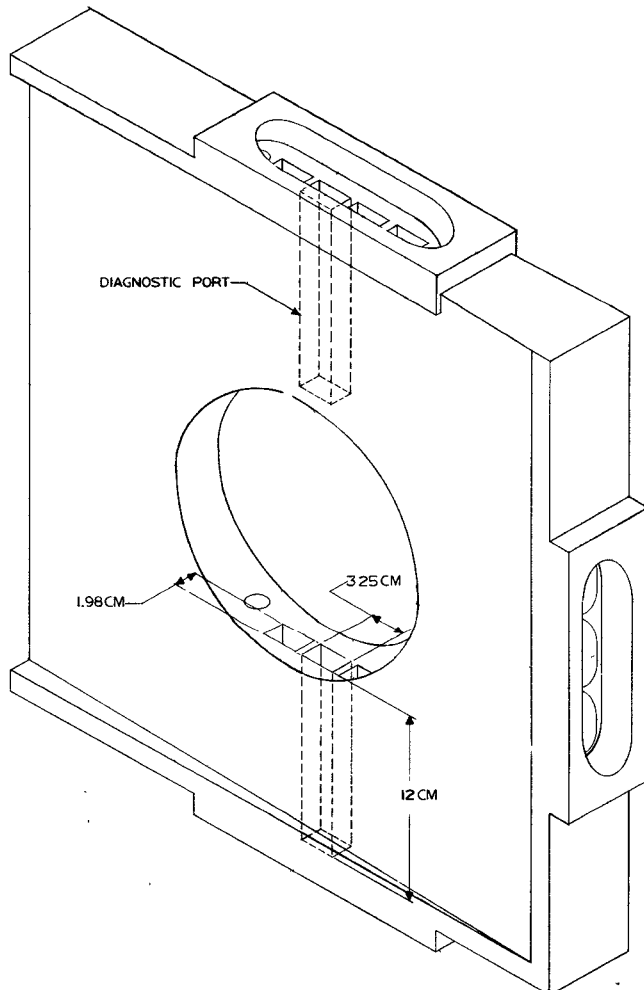
Fig. 3. Maximum angle of deviation θ_0 versus probing beam wavelength.

Fig. 4. Alcator port section.

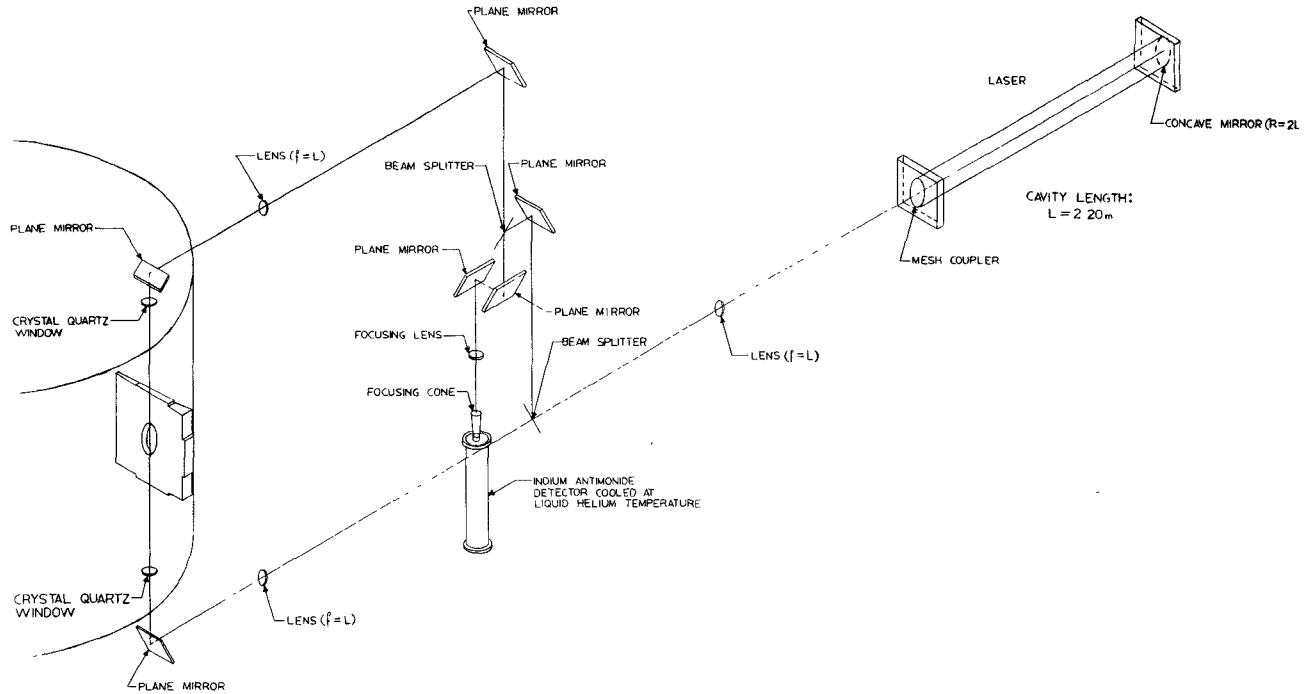


Fig. 5. Alcator HCN interferometer.

radiation source, and the interferometer itself is detailed in Subsection III-3).

1) *Description of Alcator*: Alcator is a high-field ($B = 120$ -kG) toroidal experiment. To keep the field homogeneity as high as possible, the accesses used for pumping and diagnostics have been kept as small as possible. Fig. 4 shows one of the four ports sections of the torus. To enter the long and narrow slits giving access to the plasma, the beam divergence must be smaller than 2° , the use of optical components inside the vacuum system (lenses or mirrors) being prohibited by: 1) the quality of the vacuum (the base pressure is kept below 1×10^{-8} torr), and 2) the difficulty of aligning optical elements located inside the vacuum chamber.

A high current (up to 650 kA) is induced in the plasma by means of an air core transformer. The time varying stray magnetic fluxes have several detrimental effects. First, they induce unwanted voltage transients in the cables to the detector, which therefore have to be magnetically shielded. Second, the laser has to be located far enough from the device so that the stray magnetic fields themselves do not affect the operation of the laser.

2) *The Laser*: The laser used is a semiconfocal cavity of length L , defined by a concave mirror (curvature radius $R = 2L$) on one end and a mesh coupler [6] on the other end. This method of beam extraction gives a high quality beam (small divergence, plane wave front at the exit of the cavity) and allows an easy alignment of laser in the interferometer setup. According to the well-known formula [5], the beam waist is located on the mesh coupler and its diameter is $2w_0 = 2(\lambda L/\pi)^{1/2}$. (w_0 is the $1/e$ radius of the electric field Gaussian distribution.) At $337 \mu\text{m}$, and for $L = 2.20 \text{ m}$, $w_0 = 1.54 \text{ cm}$. Horizontal parallel lines ruled on the back mirror give a linearly polarized beam (to better than 95 percent).

The stimulated emission at $337 \mu\text{m}$ occurs between

rotational energy levels of the HCN molecule. The HCN molecule is created and excited by running a 1-A dc current into a mixture of CH_4 (25 percent), N_2 (25 percent), and He (50 percent) at a pressure of $700 \mu\text{m}$. The current is regulated to better than 3 percent with a time constant of 1 ms.

3) *The Interferometer*: Fig. 5 is a general view of the interferometer. The only optical elements used are lenses and front-surface plane mirrors. The lenses (focal length $f = L$) are made out of TPX [6] which has a low coefficient of absorption at $337 \mu\text{m}$ and the same index of refraction ($n = 1.43$) at $337 \mu\text{m}$ and in the visible. The beam is periodically relayed by the lenses so that its waist is on the plasma axis. The measured beam divergence $\theta = 0.45^\circ$ is in agreement with the theoretical value [5] of 0.41° and compatible with the narrow ports (θ must be smaller than 2°). Windows are 1-cm-thick z -cut crystal quartz disks. Melinex sheets are used to split the beam. Their thickness is chosen so that the reference beam and the plasma beam reach the detector with the same intensity A . For phase adjustments, the mirrors M_1 and M_2 are mounted on translation stages. The detector is an InSb crystal immersed in a 15-kG magnetic field and cooled to liquid helium temperature. The detected signal is sent to Alcator control room, amplified, stored on a magnetic drum, and can be directly sent to an oscilloscope or processed by the on-line computer.

IV. EXPERIMENTAL RESULTS

The interferometer was tested on Alcator in May 1973 [7] and has been in regular use since April 1974. To check the density data, we choose a Tokamak regime such that the simultaneous use of a microwave interferometer was possible. The working frequency of the microwave interferometer is 84 GHz, corresponding to a cutoff

density of $8.75 \times 10^{13} \text{ cm}^{-3}$ and giving a linear phase shift for densities smaller than $3.0 \times 10^{13} \text{ cm}^{-3}$. For a parabolic density profile, this corresponds to an average density of $2.0 \times 10^{13} \text{ cm}^{-3}$.

Fig. 6 shows an interferogram obtained with the HCN interferometer (top trace). The middle trace gives the time evolution of the toroidal current and the bottom trace is the time evolution of the density, as given by the unfolding of the microwave interferogram.

The HCN interferometer is tuned so as to give maximum constructive interference at $t = 0$. The signal intensity is thus

$$I = 2A^2(1 + \cos \Delta\phi) \quad (8)$$

where $(\Delta\phi)$ is given by (5) or

$$(\Delta\phi/2\pi) = (a/\lambda_b)(\bar{n}_e/n_{co}) \quad (9)$$

where \bar{n}_e is the average density and a is the plasma radius ($a = 9 \text{ cm}$). Comparison of this interferogram with the microwave data shows a very close agreement. As the density rises rapidly at the beginning of the discharge, I decreases to zero (half a fringe) then increases again. The maximum phase shift is $\Delta\phi \simeq 1.6\pi$ corresponding to a maximum average density of $2.9 \times 10^{13} \text{ cm}^{-3}$ (at $t \simeq 19 \text{ ms}$). From there on the density decreases. The maximum average density as given by calibration of the microwave interferometer is $3.2 \times 10^{13} \text{ cm}^{-3}$. Taking into account the correction mentioned in Section II (6) this gives a peak density of $4.2 \times 10^{13} \text{ cm}^{-3}$. The HCN interferometer gives a peak density of $4.3 \times 10^{13} \text{ cm}^{-3}$, in very good agreement. Close examination of the picture shows that the HCN interferometer follows closely the small density jumps detected by the microwave interferometer.

The minimum detectable density is determined by the interferometer noise. In our setup, where all the optical elements (except the vacuum windows) are mounted on supports independent of Alcator, the vibrations are not detectable. The main source of noise arises from the laser itself; although the laser is operated in a regime where the striations of the discharge remain stable, there always remains a slight fluctuation of the last striation near the anode of the laser. This fluctuation, induces a 500-Hz ripple of the laser output. The amplitude of this modulation (1/20 of a fringe) sets the lowest limit of the linear density $\bar{n}_e d$ which can be measured with the interferometer ($\bar{n}_e d = 4.0 \times 10^{13} \text{ cm}^{-2}$); in our plasma of 18 cm in diameter, the minimum average detectable density is $2.0 \times 10^{12} \text{ cm}^{-3}$. This limit, which is already low for present day Tokamaks, will go down as the plasma size goes up in the larger experiments being built. Another way to reduce

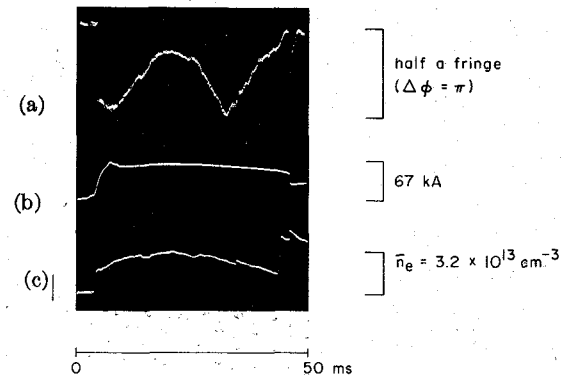


Fig. 6. Alcator density measurements. (a) 337- μm interferogram. (b) Plasma current. (c) Microwave density measurement. Experimental conditions: magnetic field $B = 20 \text{ kG}$; filling pressure $p_0 = 10^{-4} \text{ torr}$.

the minimum measurable density would be to use a double-pass (Michelson) interferometer. Attempts made to work in the Michelson configuration on Alcator have proved unsuccessful, because of the small size of the entrance ports. A Michelson interferometer would be easier to operate on an experiment with bigger ports.

CONCLUSION

Interferometry at 337 μm has been proven to be feasible and well adapted to density measurements in Tokamaks. The phase shift is a linear function of the density, throughout the range of interest for Tokamaks. Diffraction effects are neglectable. The minimum detectable linear density in the described setup is $\bar{n}_e d = 4 \times 10^{13} \text{ cm}^{-2}$.

ACKNOWLEDGMENT

P. Brossier wishes to thank P. B. Coppi and the Alcator team for their hospitality during his stay at M.I.T. He also wishes to thank Dr. D. Cohn for his contribution in the early stage of this work, and B. Geary for his technical assistance.

REFERENCES

- [1] M. A. Heald and C. B. Wharton, *Plasma Diagnostics with Microwaves*. New York: Wiley, 1965.
- [2] Alcator Group, "Plasma operations of Alcator at 'low' magnetic fields," in *Proc. 3rd Symp. Toroidal Plasma Confinement* (Garching, Germany), Mar. 1973, p. B18.
- [3] J. Shmoys, "Proposed diagnostic method for cylindrical plasmas," *J. Appl. Phys.*, vol. 32, pp. 689-695, Apr. 1961.
- [4] R. Ulrich, T. J. Bridges, and M. A. Pollack, "Variable metal mesh coupler for far infrared lasers," *Appl. Opt.*, vol. 9, pp. 2511-2516, Nov. 1970.
- [5] H. Kogelnik and T. Li, "Laser beams and resonators," *Appl. Opt.*, vol. 5, pp. 1550-1567, Oct. 1966.
- [6] G. W. Chantry, H. M. Evans, J. W. Fleming, and H. A. Gebbie, "TPX, a new material for optical components in the far-infrared spectral region," *Infrared Phys.*, vol. 9, pp. 31-33, Jan. 1969.
- [7] P. Brossier and R. A. Blanken, "Alcator's HCN interferometer," *Bull. Amer. Phys. Soc.*, vol. 18, p. 1307, Oct. 1973.